Controlling the interactions between polaritons and molecular vibrations in strongly coupled organic semiconductor microcavities

J. Chovan,[1,*] I. E. Perakis,[1] S. Ceccarelli,[2] and D. G. Lidzey[2,†]
[1]*Institute of Electronic Structure and Laser, Foundation for Research and Technology-Hellas and Department of Physics, University of Crete, Box 2208, Heraklion, Crete 71003, Greece*
[2]*Department of Physics and Astronomy, The University of Sheffield, Hicks Building, Hounsfield Road, Sheffield S3 7RH, United Kingdom*
(Received 25 June 2008; published 24 July 2008)

We study the microscopic processes that determine the dynamics of polaritons in strongly-coupled organic-semiconductor microcavities. Using a quantum kinetic theory, we show that resonant couplings and interactions between cavity photons, excitons, and localized molecular vibrations strongly affect the polariton resonance line shapes in *J*-aggregate microcavities. We use our many-body calculation to reproduce the measured polariton emission at exciton-photon resonance which is determined as a function of the Rabi-splitting energy.

DOI: 10.1103/PhysRevB.78.045320 PACS number(s): 71.36.+c, 78.30.Jw, 78.66.Qn, 78.67.−n

I. INTRODUCTION

Low-dimensional semiconductor microcavities operating in the strong-coupling regime have proved a fascinating system for studying and manipulating the coupling of light with matter.[1,2] Photons confined within the microcavity couple strongly with excitons, the elementary electronic excitations of semiconductors. This light-matter coupling results in the formation of new states termed cavity-polaritons.[3] Due to their small effective mass, cavity-polaritons have a small density of states, which permits macroscopic occupancy at relatively low excitation densities.[4] This effect has led to the observation of macroscopic quantum-mechanical phenomena, such as nonlinear stimulated scattering[5,6] and the identification of a Bose-Einstein condensate.[7]

So far, the majority of research has focused on strongly-coupled microcavities containing III–V [InGaAs/GaAs (Refs. 4 and 6) or GaN (Refs. 8 and 9)] and II–VI inorganic semiconductors.[10] Organic semiconductor microcavities have the potential of demonstrating effects not yet achievable with such inorganic semiconductors.[11,12] For example, Rabi-splitting energies in excess of 300 meV (Ref. 13) can be realized, while typical values in III–V semiconductor quantum-well microcavities do not exceed ~10 meV. Organic microcavities also offer the advantage of tunability of parameters such as the Rabi-splitting energy.[11,13] Furthermore, excitonic emission can be generated from organic light emitting diodes driven under high current stress[14] without charge-carrier screening effects becoming dominant; an effect resulting from the large ($\leq$0.5 eV) binding energy[11] of Frenkel excitons. Thus while both organic[15] and inorganic[16–18] semiconductor microcavities operating in the strong-coupling regime have been shown to emit polariton luminescence following electrical injection, it is possible that a larger population of polaritons could be generated in a strongly-coupled organic-based system via electrical injection without the system reverting to the weak-coupling limit.

It is clear however that a number of questions remain unanswered regarding the fundamental processes that occur in strongly-coupled organic microcavities; namely, whether the use of organic materials results in fundamentally new physical effects, and whether stimulated scattering can be generated. This second issue is of both fundamental and technological interest, as stimulated scattering has been proposed as a means of creating ultrafast optical switches,[19] optical-parametric amplifiers,[6] and polariton lasers.[20] It is known that new interactions are likely to be important in organic-based microcavities. For example, a special characteristic of organic systems is the strong coupling between localized Frenkel excitons (*X*s) and discrete molecular vibrational modes (VMs). Previous work argued that such interactions are likely to play a key role in polariton relaxation.[21–24] Such effects are analogous to the increase of the polariton relaxation rate due to interactions with LO phonons demonstrated in II–VI semiconductor-based microcavities.[25] Very recently, the photoluminescence (PL) emission from a strongly-coupled organic microcavity was described by a model that includes scattering with a thermal bath of vibrational modes having a continuous energy spectrum.[26] This semiclassical model reproduces the dependence of the relative PL emission intensities of the upper and lower polariton branch resonances (UPB and LPB) on the temperature, in qualitative agreement with experiment.[27]

In this paper we demonstrate that the polariton resonances in strongly-coupled organic microcavities are strongly affected by resonant exciton-molecular phonon ($X-\mathrm{VM}$) couplings, which we control by tuning the Rabi energy. We describe the cavity PL spectrum with a quantum-kinetic density-matrix calculation that employs a correlation expansion in order to treat nonperturbatively the dynamical interactions between the photons, excitons, and localized discrete vibrational modes. Importantly, the inclusion in our model of a number of discreet localized VMs (whose energies we determine from experiment) goes beyond the simplifying assumption[26] of a continuous VM distribution. In particular, we show that in addition to semiclassical relaxation effects, the resonant interactions among the discrete elementary excitations of the organic system lead to polariton normal modes consisting of a superposition of *X*s, VMs, and photons. Such quantum-mechanical effects manifest themselves in the line shapes of the UPB and LPB resonances. Our calculations suggest that, when the $\mathrm{UPB}-X$ energy separation approaches the energy of a discrete VM, the coupling between the $\mathrm{UPB}-X+\mathrm{VM}$ and $X-\mathrm{LPB}+\mathrm{VM}$ states becomes

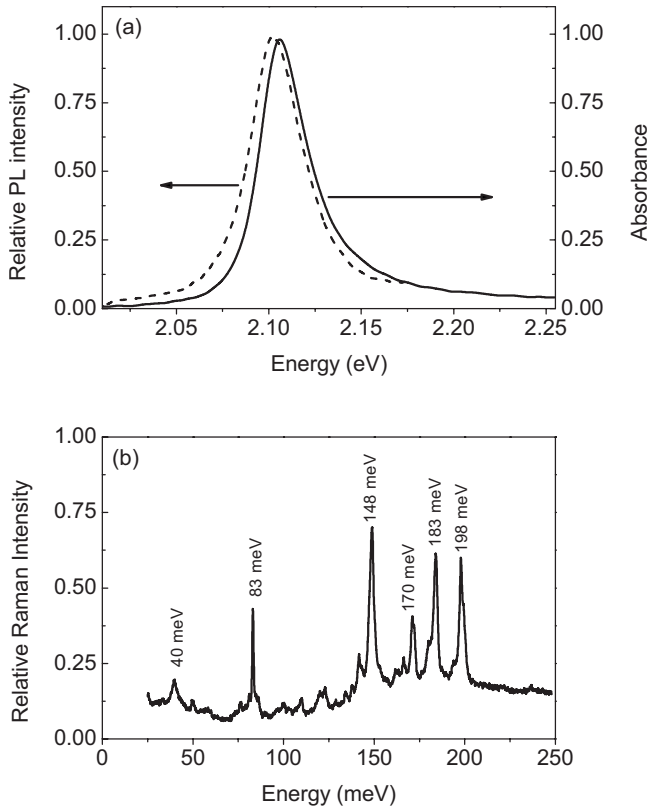

FIG. 1. (a) PL and absorption spectra of thin control film of *J* aggregates. (b) Raman spectrum of *J* aggregates of dye F1 dispersed in gelatine.

strong and modifies the polariton eigenstates and normal-mode energies (polaronic effects). We pinpoint the importance of this fundamental many-body process by studying the dependence of the relative PL emission intensity of the UPB and LPB on the Rabi-splitting energy, measured by comparing a series of organic microcavities. We find a suppression of the UPB and enhancement of the LPB PL resonance whose dependence on the Rabi-splitting energy is reproduced well by the theory.

II. EXPERIMENTAL METHODS

The cavities that we have studied are based on a thin film of a *J*-aggregated molecular dye which is positioned between a dielectric mirror (nine repeat pairs of SiO_2/Si_xN_y) and a metallic mirror consisting of a silver film deposited via thermal evaporation. Typical cavities had a *Q* factor of around 80—a value typical of microcavities that utilize at least one metallic mirror.[11] The molecular dye used in the cavities was supplied by FEW Chemicals GmbH, catalog reference S0046 and henceforth referred to as F1. To process dye F1 into a thin film and generate *J* aggregates, it was dissolved at a concentration between 1 and 4 mg/ml in a 5% water solution of gelatine and then spin cast into thin films having a thickness of 200 nm. Unlike in inorganic systems, here the Rabi-splitting energy can be tuned almost continuously by controlling the dye concentration and thus the effective oscillator strength of the organic film within the cavity.[13,28] Figure 1(a) shows the absorption and photoluminescence of a thin film of F1 *J* aggregates without the cavity. This spectrum is dominated by the strong absorption of the exciton *J* band at 2.11 eV; there is a Stokes shift of 3.9 meV between absorption and PL.

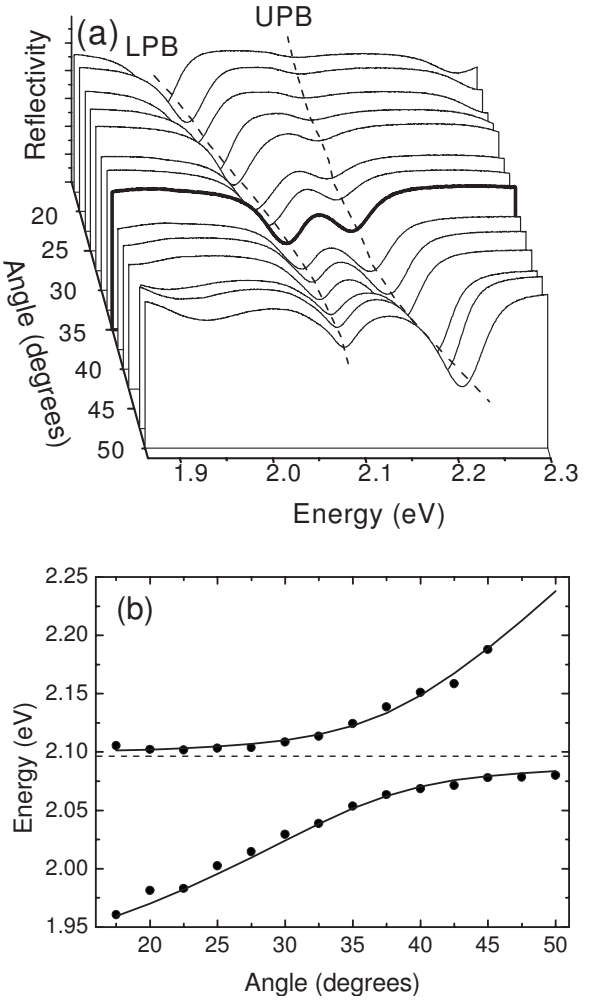

FIG. 2. Angle-resolved white-light reflectivity spectra from a microcavity with Rabi splitting of 70 meV. Thicker line: spectrum at resonance (35°). (b) Polariton dispersion extracted from (a). Solid line: best fit to a standard two-level model.

The vibrational modes of the F1 aggregates were characterized by Raman spectroscopy using a Renishaw Raman imaging microscope (operating at 633 nm). Control measurements demonstrated that the Raman-scattered modes originated from the *J* aggregates and not the matrix material. Figure 1(b) shows a typical Raman spectrum of *J* aggregates of F1 in gelatine; it is dominated by *discrete* peaks due to local molecular vibrations.

III. EXPERIMENTAL RESULTS

Figure 2(a) shows a series of white-light reflectivity spectra from a typical cavity. By plotting the energy of the dips in the reflectivity, we construct the dispersion curve of Fig. 2(b). Anticrossing is clearly observed, with (in this case) a Rabi-splitting energy of 70 meV (determined at an external

viewing angle defined with respect to the cavity normal of 35°). We fitted the energy of the polariton peaks in Fig. 2(a) to a standard two-level model[4] and identified the external viewing angle at which exciton-photon resonance occurs.

We now turn to the PL spectrum and its evolution with the Rabi-splitting energy. PL was generated following nonresonant excitation at normal incidence using the 408 nm line from a GaN laser diode focused to a 150 μm diameter spot on the cavity surface at a power density of 140 kW/m^2, and then collected over a solid angle of 0.022 *sr* using a lens and delivered into a charge coupled device spectrograph via an optical fiber. Figure 3(a) shows a series of experimental PL spectra from different microcavities, all recorded at exciton-photon resonance (corresponding to external viewing angles typically between 32.5° and 37.5°). These cavities differ in their Rabi-splitting energies (58, 70, 110, and 137 meV). With the *X* and the cavity photon in resonance (zero detuning), the UPB and LPB polaritons both contain the same cavity photon fraction, and are simultaneously sensitive to their interactions with the vibrational modes, which occur via their excitonic component.

Figure 3(a) demonstrates that, for low Rabi-splitting energies (<60 meV) as determined from the reflectivity, the cavity PL emission is dominated by an asymmetric resonance with a high energy shoulder. For larger Rabi splittings, there are two resolvable emission peaks. For the highest Rabi energy measured (137 meV), a third peak is visible. This corresponds to the PL peak of the *J* aggregate without the cavity and originates from *X*s uncoupled to the cavity photon. Due to the disorder, the majority of states in organic cavities are *X*s that do not couple significantly to this photon and form an *X* reservoir.[21] We identify the UPB with the dashed line in Fig. 3(a). For cavities where there is a small Rabi-splitting energy (where only one asymmetric PL peak is observed in emission) it is difficult to unambiguously identify the energy of the upper polariton branch. We have therefore used the energy of the upper polariton branch determined from reflectivity to estimate the position and intensity of the unresolved upper polariton in the PL emission spectrum as shown in Fig. 3(a). For these cavities, the Rabi-splitting energy is estimated from the energy separation between UPB and LPB determined from reflectivity. For larger Rabi-splitting energies, where both polariton branches are resolvable in the PL emission spectrum, we identified their position from the emission spectrum following a fit with two Lorentzian functions. The Rabi-splitting energy was then identified with the separation between the two polariton peaks in the PL spectrum.

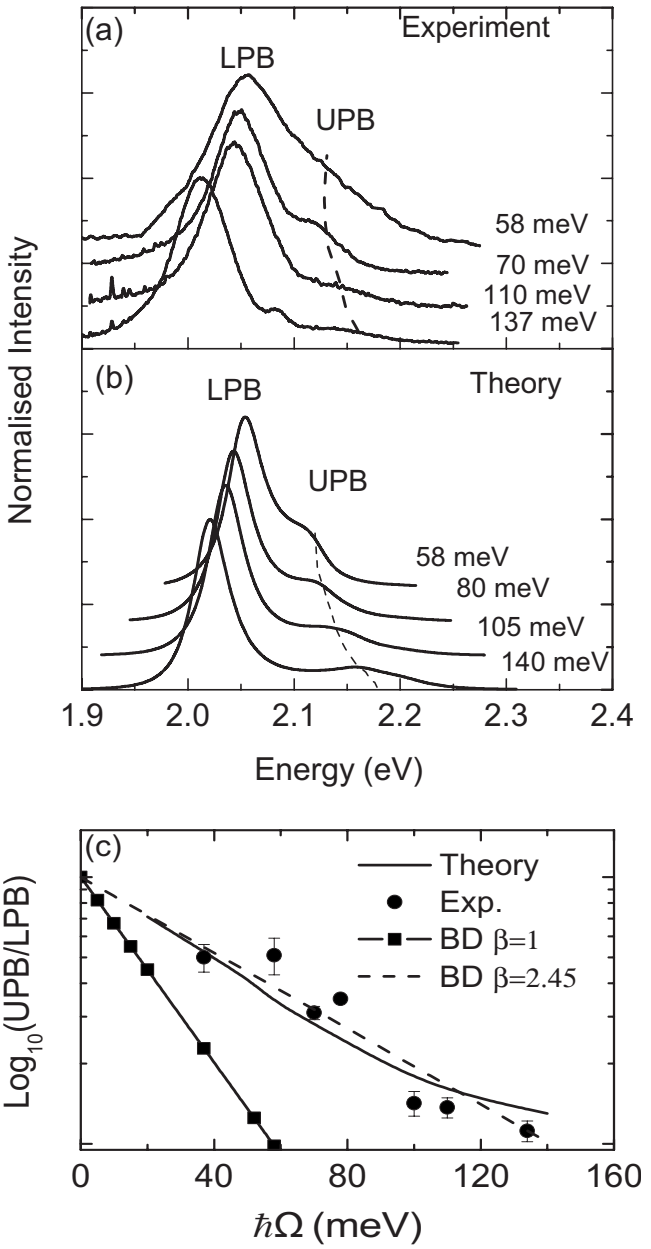

FIG. 3. PL spectra from microcavities with different Rabi-splitting energies $\hbar\Omega$: (a) Experiment, (b) theory, and (c) ratio of UPB to LPB intensities. Symbols: experiment, Solid line: theory. Also shown is the Boltzmann distribution result $I_{\mathrm{UPB}}/I_{\mathrm{LPB}}=\exp(\hbar\Omega/\beta k_B T)$, $T=300$ K, and $\beta=1.0, 2.45$.

IV. THEORY

The many-body processes induced by the interplay between $X-\mathrm{VM}$ and *X*-photon interactions were described with a quantum-mechanical theory based on density-matrix equations of motion.[29,30] We adopted the quasimode approximation, which considers external (emitted) photons coupled to cavity photons with the same in-plane vector and polarization, and used the simplest Hamiltonian[21] that describes the interactions between cavity photons, molecular phonons, and molecular excitons. $a_{\mathbf{q}}^{\dagger}$ creates the lowest cavity photon, with in-plane momentum $\mathbf{q}$ and energy $\Omega_{\mathbf{q}}$,[21] $B_m^{\dagger}$ creates a molecular exciton, with energy Ω_X, and $c_m^{\dagger}$ creates an intramolecular phonon, with energy Ω_{ph}, localized on the *m*th molecule. Given the peaks in the Raman spectra of Fig. 1(b), we included up to two discrete VMs in our calculation, whose energies are within the range of Rabi splittings studied in our experiments. The population of emitted photons can be obtained in terms of the density matrices $\langle a_{\mathbf{q}}^{\dagger}a_{\mathbf{q}'}\rangle$, $\langle B_m^{\dagger}B_n\rangle$, and $\langle a_{\mathbf{q}}^{\dagger}B_n\rangle$, which satisfy the equations of motion

$$i\partial_t\langle a_{\mathbf{q}}^\dagger a_{\mathbf{q}'}\rangle = (\Omega_{\mathbf{q}'} - \Omega_{\mathbf{q}})\langle a_{\mathbf{q}}^\dagger a_{\mathbf{q}'}\rangle + \sum_m [T_{m\mathbf{q}'}\langle a_{\mathbf{q}}^\dagger B_m\rangle - T_{\mathbf{q}m}\langle B_m^\dagger a_{\mathbf{q}}\rangle], \quad (1)$$

$$i\partial_t\langle a_{\mathbf{q}}^\dagger B_m\rangle = (\Omega_X - \Omega_{\mathbf{q}})\langle a_{\mathbf{q}}^\dagger B_m\rangle + \sum_{\mathbf{q}'} T_{\mathbf{q}'m}\langle a_{\mathbf{q}}^\dagger a_{\mathbf{q}'}\rangle - \sum_n T_{\mathbf{q}n}\langle B_n^\dagger B_m\rangle + \lambda\langle a_{\mathbf{q}}^\dagger B_m(c_m^\dagger + c_m)\rangle, \quad (2)$$

$$i\partial_t\langle B_m^\dagger B_n\rangle = i\delta_{mn}P_m + \sum_{\mathbf{q}} [T_{\mathbf{q}n}\langle B_m^\dagger a_{\mathbf{q}}\rangle - T_{m\mathbf{q}}\langle a_{\mathbf{q}}^\dagger B_n\rangle] + \lambda[\langle B_m^\dagger B_n(c_n^\dagger + c_n)\rangle - \langle B_m^\dagger B_n(c_m^\dagger + c_m)\rangle]. \quad (3)$$

In the above equations, λ denotes the X-phonon interaction constant, $T_{\mathbf{q}m}$ describes the X-photon coupling,[21] P_m is the pumping rate, and we include photon and X lifetimes. Unlike the semiclassical approximation, we describe the X-phonon interaction effects via phonon-assisted density matrices [last terms on the right-hand side of Eqs. (2) and (3)], which are determined by their own equations of motion. These equations couple to higher density matrices, primarily of the forms $\langle B^\dagger B c^\dagger c\rangle$ and $\langle a^\dagger B c^\dagger c\rangle$. The latter density matrices are decomposed into a factorizable part, where the phonon occupation number $\langle c^\dagger c\rangle$ is substituted by a thermal distribution, and a nonfactorizable contribution determined by its equation of motion. We truncated the infinite density-matrix hierarchy by neglecting the coupling to higher density matrices describing multiphonon correlations. We expect that the disorder fluctuations suppress these multi-VM correlations in organic systems. The semiclassical treatment of the $X-$VM scattering, which leads to a master equation for the populations, is recovered by solving the equations of motion of the single-phonon density matrices in the adiabatic limit.[30] Here however we treat polaronic contributions to the PL spectra, due to the hybrid X, photon, and phonon nature of the polariton eigenstates, by solving the above system of equations and their coupling to the external photons numerically in the steady state, assuming an initial X population $\langle B_m^\dagger B_m\rangle$. More details will be presented elsewhere.

V. DISCUSSION

Figure 3(b) shows the trends in the PL spectra, calculated for zero exciton-photon detuning and zero temperature, as function of Rabi energy. The free parameters (λ and relaxation rates) were fixed by fitting to the details of the experimental PL line shape for one Rabi energy; they were then kept constant for all other Rabi energies. The VM energies were extracted from the Raman spectra. The theory reproduces very well the experimental trends with Rabi energy tuning. The UPB is suppressed and broadened asymmetrically (non-Lorentzian line shape) by the X-phonon interaction, which also enhances the LPB resonance. In fact, due to the polaronic effects and the coupling of the $X+$VM and UPB states, we can even obtain two split UPB peaks, which however merge into a single broad resonance due to the rather large damping rates. Importantly, the above effects depend on the relative values of the discrete molecular vibration frequencies as compared to the energy splitting of the polariton states. In particular, the contribution to the normal modes coming from the coupling of Xs and VMs diminishes as the $X+$VM and polariton energies get out of resonance. These energy differences can be tuned by changing the Rabi energy, which thus controls the PL line shape.

In Fig. 3(c) we plot the experimental ratio of the UPB to LPB intensity as a function of Rabi-splitting energy (solid points). In each case, the measurement was repeated on at least three independent microcavities. It is clear that the relative intensity UPB/LPB decreases strongly with increasing Rabi-splitting energy. This trend can already be seen from the PL resonance line shapes in Fig. 3(a) and does not depend on our fitting procedure. Our calculation gives good agreement with this experimental result if we include the two dominant molecular vibrations in the Raman spectrum, at 40 and 83 meV [Fig. 1(b)], whose energy is within the range of Rabi energies considered here. If our model only includes a single VM, the theory predicts a minimum in the UPB/LPB intensity ratio as the Rabi splitting approaches about twice of the VM energy. Note that we exclude interactions with the higher lying VMs (at 148, 170, 183, and 196 meV) for the sake of simplicity since such modes are out of resonance with the X-polariton energy difference. Indeed, over the range of Rabi-splitting energies explored here (30–140 meV), the role of such high energy phonons on the relaxation from the UPB to the reservoir will be minimal, as their energy is more than twice that of the energy separation between the UPB (at maximum Rabi splitting) and the X reservoir states.

In Fig. 3(c), we also compare the Boltzmann distribution for $T=300$ K (as in the experiment) with the UPB/LPB ratio as function of Rabi-splitting energy. The clear discrepancy between the two curves shows that the two polariton branches are not in thermal equilibrium. Instead, we find that we can approximately describe the measured Rabi energy dependence of the UPB/LPB peak ratio by a Boltzmann distribution with excitation energy $\sim\frac{1}{2.45}$ of the Rabi splitting. Since this energy is comparable to the splitting between the UPB and X reservoir states, we can infer that the UPB population has a component determined by the thermal population of UPB states via X reservoir states. Indeed, the X reservoir can reach quasiequilibrium very rapidly,[24] and thus the increase in temperature creates a thermal VM population that enhances X scattering to the UPB. This picture is also supported by temperature dependent PL emission measurements on the intensity emission ratio of the UPB and LPB made on F1 dye containing microcavities.[27] In contrast, the LPB lies below the X reservoir energy and its population is mainly determined by the nonthermal part of the density matrices. Such temperature effects can be described with our theory by substituting a phonon population $\langle c_m^\dagger c_m\rangle$ in the density-matrix equations of motion.

VI. CONCLUSIONS

In summary, by combining a comprehensive experimental study of the PL spectrum of J-aggregate microcavities in the

strong-coupling regime with tunable Rabi energy and a quantum kinetic many-body calculation, we have demonstrated the crucial role played by resonant exciton-molecular vibration interactions in organic microcavities. Our results highlight the suggestion[24] that, if the energy separation between the exciton reservoir and the minimum of the lower-branch polariton energies can be tuned to be resonant with the energy of a vibrational mode, rapid and efficient macroscopic occupancies of this LPB state may be achieved following nonresonant exciton excitation, potentially leading to stimulated-scattering effects in organic microcavities. Furthermore recent theoretical work suggests that polariton-polariton kinematic interactions in organic microcavities can result in a range of nonlinear effects, such as parametric scattering.[31] It is however likely that the generation of such nonlinear effects will only be possible in structures having a significantly higher Q factor (which is directly related to the cavity photon lifetime) than those studied here. Such increases in cavity Q factor can be readily achieved by creating structures based on two distributed Bragg reflectors,[32] or by creating microcavities based on a micropillar-type geometry.[33]

ACKNOWLEDGMENTS

This work was supported by the European Commission via the 5th Framework research training network HYTEC Contract No. HPRN-CT-2002-00315.

*ilias@physics.uoc.gr
†d.g.lidzey@sheffield.ac.uk

[1] C. Weisbuch, M. Nishioka, A. Ishikawa, and Y. Arakawa, Phys. Rev. Lett. **69**, 3314 (1992).
[2] G. Khitrova, H. M. Gibbs, F. Jahnke, M. Kira, and S. W. Koch, Rev. Mod. Phys. **71**, 1591 (1999).
[3] J. J. Hopfield, Phys. Rev. **112**, 1555 (1958).
[4] M. S. Skolnick, T. A. Fisher, and D. M. Whittaker, Semicond. Sci. Technol. **13**, 645 (1998).
[5] P. Senellart and J. Bloch, Phys. Rev. Lett. **82**, 1233 (1999).
[6] R. M. Stevenson, V. N. Astratov, M. S. Skolnick, D. M. Whittaker, M. Emam-Ismail, A. I. Tartakovskii, P. G. Savvidis, J. J. Baumberg, and J. S. Roberts, Phys. Rev. Lett. **85**, 3680 (2000).
[7] J. J. Kasprzak *et al.*, Nature (London) **443**, 409 (2006).
[8] N. Antoine-Vincent, F. Natali, D. Byrne, A. Vasson, P. Disseix, J. Leymarie, M. Leroux, F. Semond, and J. Massies, Phys. Rev. B **68**, 153313 (2003).
[9] R. Butté, G. Christmann, E. Feltin, J. F. Carlin, M. Mosca, M. Ilegems, and N. Grandjean, Phys. Rev. B **73**, 033315 (2006).
[10] R. André and L. S. Dang, J. Appl. Phys. **82**, 5086 (1997).
[11] D. G. Lidzey, D. D. C. Bradley, M. S. Skolnick, T. Virgili, S. Walker, and D. M. Whittaker, Nature (London) **395**, 53 (1998).
[12] R. J. Holmes and S. R. Forrest, Phys. Rev. Lett. **93**, 186404 (2004).
[13] P. A. Hobson, W. Barnes, D. G. Lidzey, G. A. Gehring, D. M. Whittaker, M. S. Skolnick, and S. Walker, Appl. Phys. Lett. **81**, 3519 (2002).
[14] C. I. Wilkinson, D. G. Lidzey, L. C. Palilis, R. B. Fletcher, S. J. Martin, X. H. Wang, and D. D. C. Bradley, Appl. Phys. Lett. **79**, 171 (1999).
[15] J. R. Tischler, S. M. Bradley, V. Bulović, J. H. Song, and A. Nurmikko, Phys. Rev. Lett. **95**, 036401 (2005).
[16] L. L. Sapienza, A. Vasanelli, R. Colombelli, C. Ciuti, Y. Chassagneux, C. Manquest, U. Gennser, and C. Sirtori, Phys. Rev. Lett. **100**, 136806 (2008).
[17] D. Bajoni, E. Semenova, A. Lemaître, S. Bouchoule, E. Wertz, P. Senellart, and J. Bloch, Phys. Rev. B **77**, 113303 (2008).
[18] A. A. Khalifa, A. P. D. Love, D. N. Krizhanovskii, M. S. Skolnick, and J. S. Roberts, Appl. Phys. Lett. **92**, 061107 (2008).
[19] M. Saba *et al.*, Nature (London) **414**, 731 (2001).
[20] S. Christopoulos *et al.*, Phys. Rev. Lett. **98**, 126405 (2007).
[21] V. M. Agranovich, M. Litinskaia, and D. G. Lidzey, Phys. Rev. B **67**, 085311 (2003).
[22] D. G. Lidzey, A. M. Fox, M. D. Rahn, M. S. Skolnick, V. M. Agranovich, and S. Walker, Phys. Rev. B **65**, 195312 (2002).
[23] V. M. Agranovich, H. Benisty, and C. Weisbuch, Solid State Commun. **102**, 631 (1997).
[24] M. Litinskaya, P. Reineker, and V. M. Agranovich, J. Lumin. **110**, 364 (2004).
[25] F. Boeuf, R. André, R. Romestain, L. S. Dang, E. Peronne, J. F. Lampin, D. Hulin, and A. Alexandrou, Phys. Rev. B **62**, R2279 (2000).
[26] P. Michetti and G. C. La Rocca, Phys. Rev. B **77**, 195301 (2008).
[27] S. Ceccarelli, J. Wenus, M. S. Skolnick, and D. G. Lidzey, Superlattices Microstruct. **41**, 289 (2007).
[28] D. G. Lidzey, D. D. C. Bradley, T. Virgili, A. Armitage, M. S. Skolnick, and S. Walker, Phys. Rev. Lett. **82**, 3316 (1999).
[29] F. Rossi and T. Kuhn, Rev. Mod. Phys. **74**, 895 (2002).
[30] V. M. Axt and S. Mukamel, Rev. Mod. Phys. **70**, 145 (1998).
[31] H. Zoubi and G. C. La Rocca, Phys. Rev. B **72**, 125306 (2005).
[32] L. G. Connolly, D. G. Lidzey, R. Butté, A. M. Adawi, D. M. Whittaker, M. S. Skolnick, and R. Airey, Appl. Phys. Lett. **83**, 5377 (2003).
[33] A. M. Adawi *et al.*, Adv. Mater. (Weinheim, Ger.) **18**, 742 (2006).